Journal of Engineering Science and Technology
Vol. 14, No. 6 (2019) 3597 - 3615

DESIGN AND ANALYSIS OF A HYBRID POWER CONVERTER

MUDADLA DHANANJAYA*, SWAPNAJIT PATTNAIK

Department of Electrical Engineering, National Institute of Technology,
Raipur, Chhattisgarh, India, 492010
*Corresponding Author: krishnadhanu9390@gmail.com

Abstract

Hybrid converters have aroused significant attention in performing the multiple operations in a single converter. Further, it gives the economic operation and improves system performance. In this study, a new structure of hybrid power converter is proposed. It is formed by the simple switching structure and it can operate different modes of operation in DC-DC conversions, such as boost, buck and buck-boost mode. Similarly, in DC-AC conversion it gives better Total Harmonic Distortion (THD). The proposed hybrid converter is simulated in MATLAB/SIMULINK environment. Low power prototype circuit is developed and experimental results are validated with simulation results.

Keywords: DC-AC converters, DC-DC converters and hybrid converters.

1. Introduction

Hybrid converters (HYCs), has the following advantages over conventional solutions [1-4] that employ multiple single converters such as 1) lower cost characteristic because of sharing the reactive components and controlled switches. 2) Compact in size 3) High power density. Therefore, HYCs are good choice for nanogrid, electric vehicle (EVs) and photovoltaic applications, which is economic and therefore has good development prospects [5-7].

The HYCs are two types, such as isolated HYCs and non-isolated HYCs DC-DC converters. In isolated HYCs, converters are good candidates for the applications where galvanic isolation is required. However, the major problem is that too many active power switches are used, conversion efficiency gets lowered due to leakage losses, induces high voltage stress in the controlled switches. Similarly, the use of the transformer makes it massive [8-10].

Khan and Chowdhury [11] mentioned that multi-inductor voltage multiplier cell-based boost hybrid converter is proposed for high gain applications. However, it may not be performing the buck-boost operation. Axelrod et al. [12] suggested the switched inductor to the switched capacitor-based hybrid converter. It can improve the performance of the converter when the active switch ON period the inductors are charged in series and capacitors are discharged in parallel. Similarly, inactive switch OFF period, inductors are discharged in parallel and capacitors are charged in series.

Nevertheless, more device count, which leads, to increase the cost and the size of the converter. Bagewadi and Dambhare [13] and Harfman-Todorovic et al. [14] presented the new hybrid converter topology for nanogrid applications and fuel application. Dogga et al. [15], Siddhartha and Hote [16], Tomy and Thomas [17] and Sarath and Kanakasabapathy [18] introduced the conventional DC-DC converter based hybrid converters. These are effectively eliminating the shoot problems and, which is for suitable for nanogrid applications. Kim et al. [19] reported that the phase-shifted full-bridge (PSFB) based hybrid converter is suggested for electric vehicle chargers application. Although in this configuration, overcome the drawbacks of the conventional PSFB converter such as output filter, conduction losses and narrow zero voltage switching range. Kim et al. [20] introduced the hybrid dual full-bridge DC-DC converter for radiofrequency application.

Moreover, it overcomes the drawbacks of a conventional PSFB converter such as the size of the output filter and circulating currents. Zhang et al. [21] presented the hybrid step-down power factor correction (PFC) converter. It is combining the features of boost PFC and bucks PFC converter. In addition, improves the peak current control scheme, which results achieve a high power factor. Vecchia et al. [22] proposed that switched capacitor-based hybrid DC-DC converter and it is derived from different types of converters, such as boost, buck, and buck-boost. It has the capability of achieving a high voltage gain with increased switched capacitor cell. However, a number of capacitors cause extra cost and big size.

In this paper, a hybrid converter is introduced, which consist of the DC-DC converter and H-bridge network. It can perform the DC-DC conversion and DC-AC conversion. In inverter operation, it gives better THD%. This paper is structured as follows. In Section 2, the proposed topology and different modes of operations are

discussed and parameter design is presented in Section 3. Section 4 gives the simulation and experimental results in different configurations followed by a conclusion in Section 5.

2. Operating Principle and Different Configurations of Proposed Converter

Hybrid converters are a relatively new class of power converters. These are single-stage converters and can be configured as a DC-DC converter with H-bridge network for hybrid power conversion applications. The schematic diagram of the proposed is shown in Fig. 1. Different configurations of the proposed converter are described in detail, corresponding equivalent circuits are shown and the voltage across the capacitor and current flows through the inductor are presented.

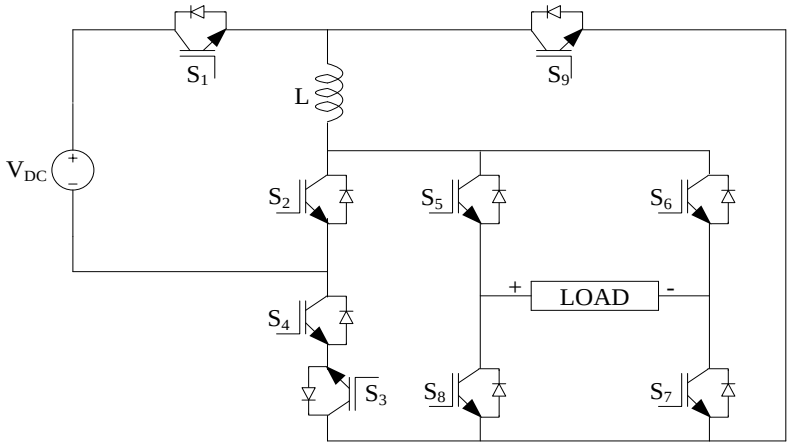

Fig. 1. Proposed converter configuration.

2.1. DC-DC converter

2.1.1. Buck mode

Mode 1

In this operating mode, the switching action happens between the switches S_1, S_4, S_5, S_7, and the reaming switches are turned OFF. In this mode, source port V_{DC} supplies the energy to the load and inductor is energized. The corresponding equivalent circuit is shown in Fig. 2(a).

The current flows through an inductor current (i_L) and voltage across capacitor (v_C) equations as follows:

$$i_L(t) = \frac{V_{DC}}{R} + e^{-\alpha t}\left[c_1 \cos \omega_d t + c_2 \sin \omega_d t\right] \tag{1}$$

$$v_C(t) = V_{DC} - \frac{L}{2C} e^{-\alpha t}\left[\begin{array}{l} \cos \omega_d t\left(\frac{\alpha c_1}{R} + \omega_d c_2\right) + \\ \sin \omega_d t\left(-\alpha c_2 + \frac{\omega_d c_1}{R}\right) \end{array}\right] \tag{2}$$

Mode 2

In this mode, the input supply is off and inductor L is delivered its stored energy to the load resistance R through the active switches S_5, S_7, and S_9. Inductor current (i_L) and voltage across the capacitor (v_C) equations in this state as follows.

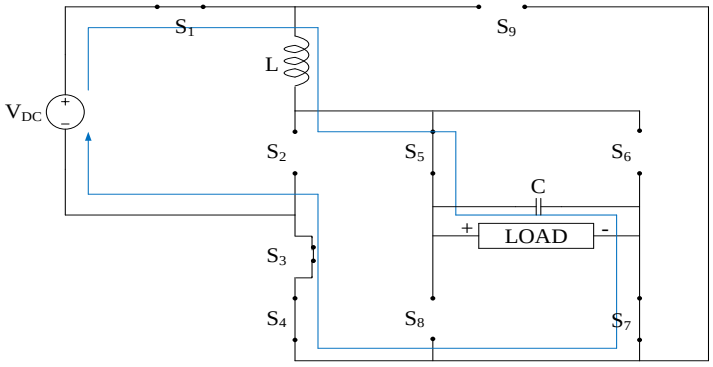

(a) Mode 1.

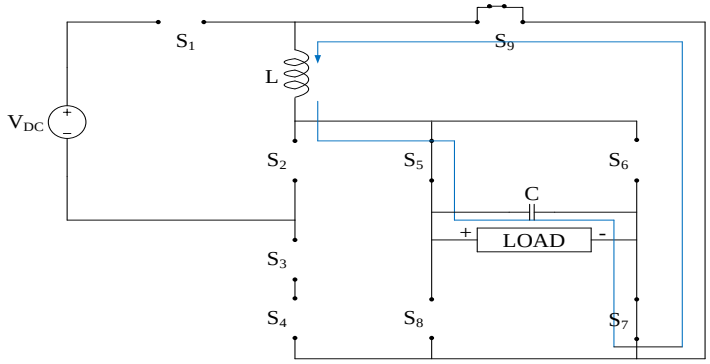

(b) Mode 2.

Fig. 2. Equivalent circuits in buck mode.

$$i_L(t) = e^{-\alpha t}\left[c_3 \cos \omega_d t + c_4 \sin \omega_d t\right] \tag{3}$$

$$v_C(t) = -Le^{-\alpha t}\begin{bmatrix}(-\alpha c_3 + \omega_d c_4)\cos \omega_d t + \\ (\omega_d c_3 - \alpha c_4)\sin \omega_d t\end{bmatrix} \tag{4}$$

where

$$\alpha = \frac{1}{2RC} \tag{5}$$

$$\omega_d = \frac{1}{2}\sqrt{\left(\frac{1}{R^2C^2} - \frac{4}{LC}\right)} \tag{6}$$

The values of c_1, c_2, c_3 and c_4 are obtained from the initial conditions.

The output voltage (V_0) expression of the proposed converter in buck mode.

$$V_0 = dV_{DC} \tag{7}$$

where '*d*' is the duty cycle of the switch.

2.1.2. Boost operation

Mode 1

In this state, active switches S_1, S_2 are turned ON and the equivalent circuit in this mode is shown in Fig. 3(a). In this mode, the voltage source charges the inductor and capacitor is delivering its stored energy to the load resistance R.

Current flows through an inductor (i_L) and the voltage across the capacitor (v_C) as follows:

$$i_L(t) = \frac{V_{DC}}{L}t + i_{L(0)} \tag{8}$$

$$v_C(t) = v_{C(0)}e^{\frac{-1}{RC}t} \tag{9}$$

Mode 2

The equivalent circuit in this state is shown in Fig. 3(b). During this mode, energy stored inductor is discharged and delivers its stored energy to the capacitor C and load R through the switches S_1, S_4, S_5, S_7, respectively.

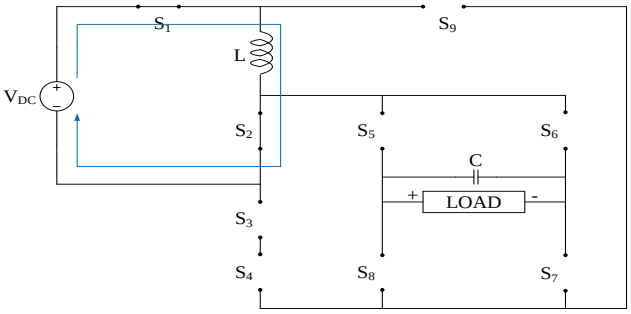

(a) Mode 1.

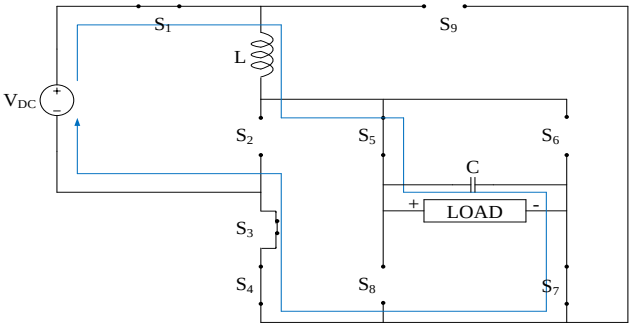

(b) Mode 2.

Fig. 3. Equivalent circuits in boost mode.

Current flows through an inductor and voltage across the capacitor as follows:

$$i_L(t) = \frac{V_{DC}}{R} + e^{-\alpha t}\left[c_1 \cos \omega_d t + c_2 \sin \omega_d t\right] \tag{10}$$

$$v_C(t) = V_{DC} - \frac{L}{2C} e^{-\alpha t}\begin{bmatrix} \cos \omega_d t(\frac{\alpha c_1}{R} + \omega_d c_2) + \\ \sin \omega_d t(-\alpha c_2 + \frac{\omega_d c_1}{R}) \end{bmatrix} \tag{11}$$

The values of c_1 and c_2 obtained from the initial conditions. Output voltage expression of the proposed converter in boost mode.

$$V_0 = \frac{V_{DC}}{(1-d)} \tag{12}$$

where '*d*' is duty cycle of the switch.

2.1.3. Buck-boost mode

Mode 1

In this mode, controlled switches S_1, S_2 are turned ON and magnetizing inductor L is energized by the input supply V_{DC} is illustrated in Fig. 4(a). Similarly, the capacitor is releasing its stored energy to the load resistance R.

The current flows through an inductor current (i_L) and voltage across capacitor (v_C) equations are as follows:

$$i_L(t) = \frac{V_{DC}}{L} t + i_{L(0)} \tag{13}$$

$$v_C(t) = v_{C(0)} e^{\frac{-1}{RC}t} \tag{14}$$

Mode 2

In this state, energy stored in inductor L is released to the load resistance R through the switches S_5, S_7, and S_9. The corresponding equivalent circuit is depicted in Fig. 4(b). The voltage across the capacitor and current flows through an inductor equation can be expressed as follows:

$$i_L(t) = e^{-\alpha t}\left[c_1 \cos \omega_d t + c_2 \sin \omega_d t\right] \tag{15}$$

$$v_C(t) = -Le^{-\alpha t}\begin{bmatrix} (-\alpha c_1 + \omega_d c_2)\cos \omega_d t + \\ (\omega_d c_1 - \alpha c_2)\sin \omega_d t \end{bmatrix} \tag{16}$$

The values of c_1 and c_2 obtained from the initial conditions.

Output voltage expression of the proposed converter in buck-boost operation as follows:

$$V_0 = \frac{V_{DC} d}{(1-d)} \tag{17}$$

where '*d*' is the duty cycle of the switch.

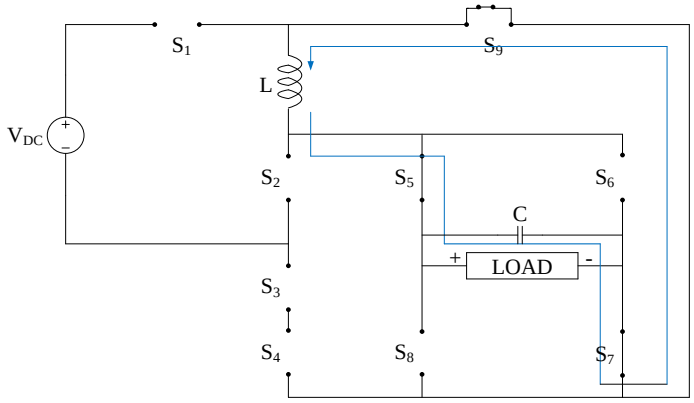

(a) Mode 1.

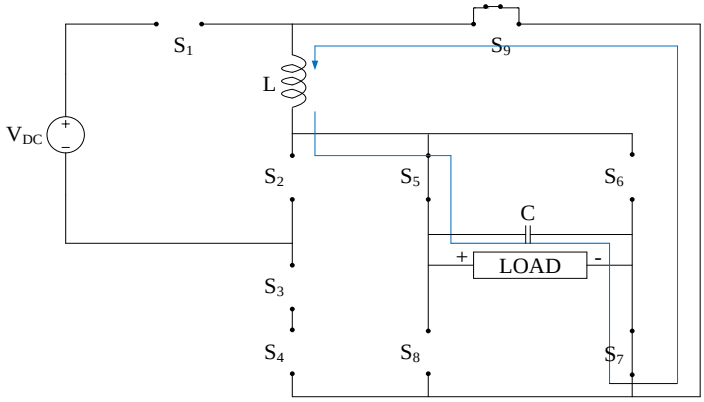

(b) Mode 2.

Fig. 4. Equivalent circuits of proposed converter in buck-boost mode.

2.2. Inverter operation

The proposed topology is operated in inverter configuration, the corresponding mode of operation and equivalent circuits are shown in Fig. 5. It is obtained from the conventional DC-DC converter and H-bride network. In this structure, suggested the approach gives better THD%.

Mode 1

In this mode, switch S_1, S_5, S_7, and S_4 are turned ON and the inductor is energized by the source port. The corresponding equivalent circuit is shown as follows.

Mode 2

In this state, supply voltage remains OFF energy stored inductor is de-energized through the switches S_5, S_7 and switch S_9. The corresponding equivalent circuit is shown below. Mode 1 and Mode 2 are generating a positive level of the output voltage.

Mode 3

In this mode, switches S_1, S_6, S_8, and S_4 are turned ON and the inductor is energized by the input voltage. The corresponding equivalent circuit is shown below.

Mode 4

In this state, energy stored inductor is de-energized through the switches S_6, S_8 and switch S_9. The corresponding equivalent circuit is shown below. Modes 3 and 4 are generating the negative level of the output voltage.

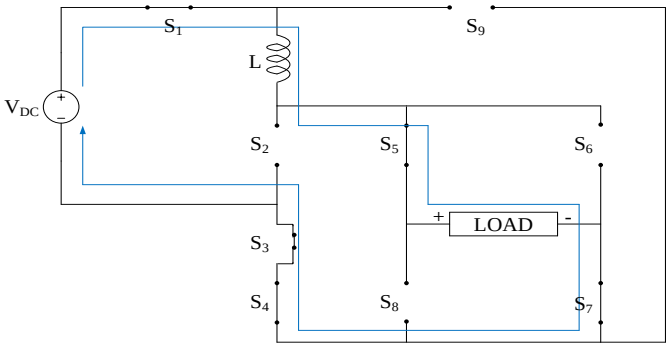

(a) Mode 1.

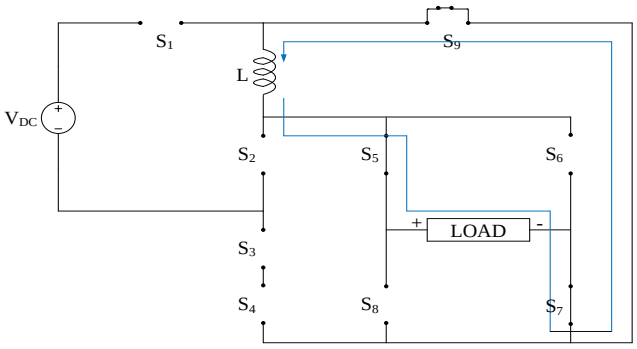

(b) Mode 2.

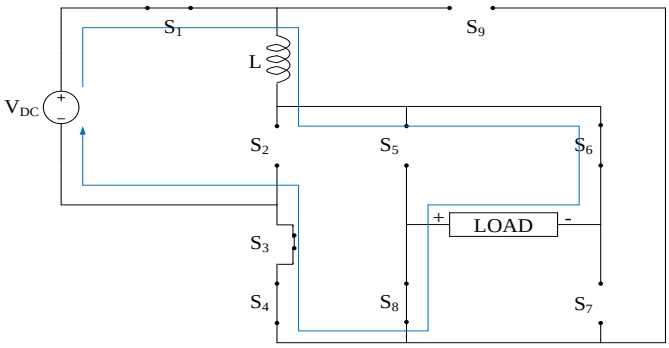

(c) Mode 3.

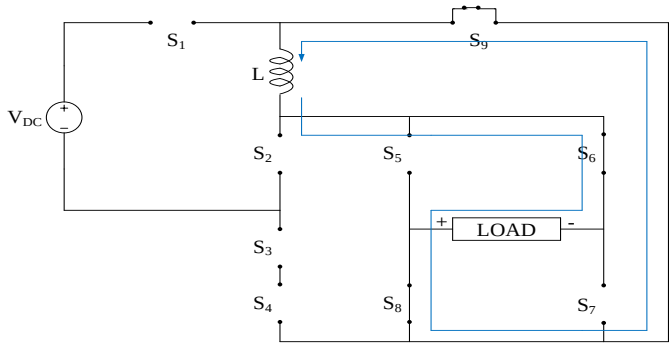

(d) Mode 4.

Fig. 5. Operating modes of proposed converter in inverter configuration.

Output voltage

$$V_{rms} = \sqrt{\left[\frac{1}{T}\int_0^t V_{DC}^2 dt\right]} \tag{18}$$

$$V_{rms}^2 = \frac{V_{DC}^2}{T}\left[\begin{array}{l} d_1 T + \frac{L}{2R} + \frac{2L}{R} e^{\frac{-d_1 TR}{L}} - \\ \frac{2L}{R} - \frac{L}{2R} e^{-(\frac{d_1+d_2}{L})R} \end{array}\right] \tag{19}$$

3. Parameters Design

The circuit design considerations mainly depend on magnetic components, capacitors, duty ratio, type of switches and switching frequency. Even though inductors and transformers are both magnetic components, there is a very important difference in their functioning and design aspect [23].

Step 1. Calculation of maximum and minimum power.

$$\begin{aligned} P_{0\max} &= V_0 I_{0\max} \\ P_{0\min} &= V_0 I_{0\min} \end{aligned} \tag{20}$$

Step 2. Calculation of maximum and minimum of the load resistance.

$$R_{L\max} = \frac{V_0}{I_{0\min}}$$

$$R_{L\min} = \frac{V_0}{I_{0\max}} \tag{21}$$

Step 3. The voltage conversion ratio of the converter.

$$M_{V\ DC\min} = \frac{V_0}{V_{DC\max}}$$

$$M_{V\ DC\max} = \frac{V_0}{V_{DC\min}} \tag{22}$$

Step 4. Calculation of the duty cycle.

$$D_{\min} = \frac{M_{V\ DC\max}}{\eta}$$

$$D_{\max} = \frac{M_{V\ DC\min}}{\eta} \tag{23}$$

where 'η' is efficiency.

Step 5. Calculation of minimum inductance.

$$L_{\min} = \frac{R_{L\max}(1-D_{\min})}{2f_s} \tag{24}$$

f_s = switching frequency

Step 6. Selection an inductance L, which is grater $L_{\min}$ and $\Delta i_{L\max}$ are computed as:

$$\Delta i_{L\max} = \frac{V_0(1-D_{\max})}{f_s L} \tag{25}$$

Step 7. Calculation of filter capacitance.

$$C_{\min} = \frac{D_{\max}}{2f_s r_c} \tag{26}$$

where

$$r_{C\max} = \frac{v_r}{\Delta i_{L\max}} \tag{27}$$

4. Simulation and Experimental Results

4.1. Simulation results

The simulations are performed to evaluate the operation of the proposed converter using MATLAB/Simulink. The test was conducted in different modes such as DC-DC and DC-AC mode. The input voltage is considered 50 V, the duty cycle of 60%, switching frequency is 10 kHz, the capacitor value is 120 uF and the inductor value is chosen 5 mH. Simulation output voltage and inductor current in a step-down mode are depicted in Fig 6(a), 6(b) respectively.

In this mode, from Fig. 6(b) l_{Final} value is 2.57 A and $l_{Initial}$ value is 2.43 A. In boost and buck-boost operation, output voltage and inductor are shown in Figs. 7(a) and (b) and 8(a) and (b) respectively. In boost operation, from Fig. 7(b), l_{Final} value is 3.12 A and $l_{Initial}$ value is 2.9 A. Similarly, buck-boost mode, from Fig. 8(b), l_{Final} value is 5.01 A and $l_{Initial}$ value is 4.798 A. In inverter configuration, the input voltage is set to be 50 V and inductor value 19 mH is considered. The corresponding output voltage, load current, and FFT analysis are illustrated in Figs. 9(a) to (c) respectively.

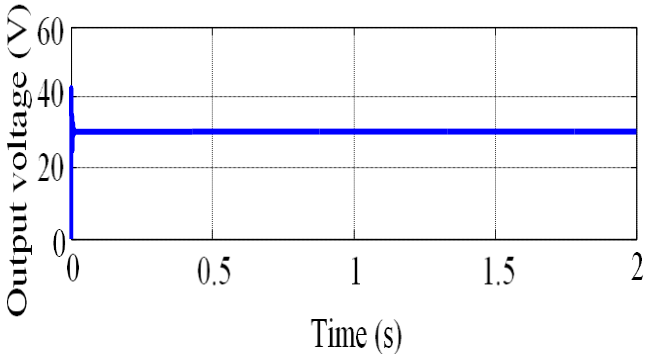

(a) Output voltage.

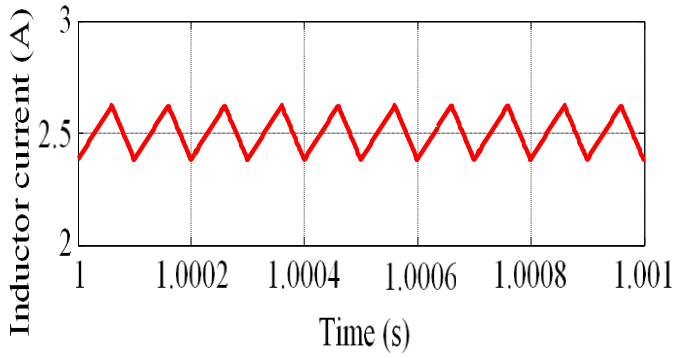

(b) Inductor current.

Fig. 6. Simulation results in buck operation.

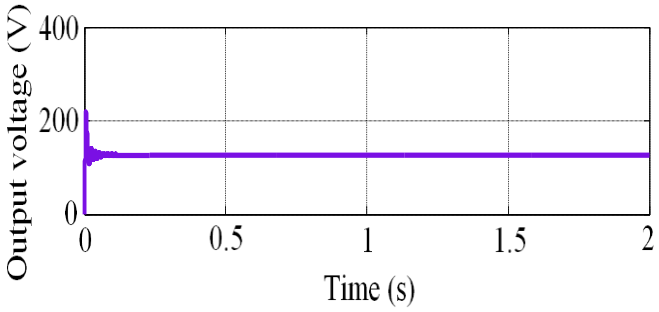

(a) Output voltage.

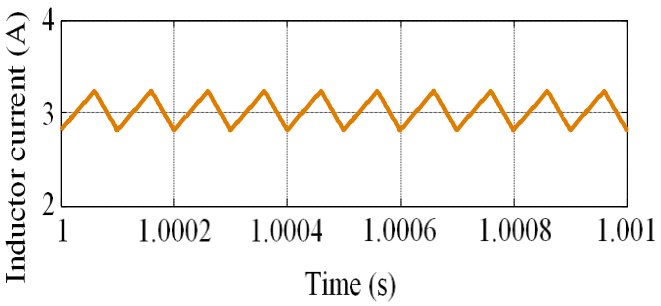

(b) Inductor current.

Fig. 7. Simulation results in boost operation.

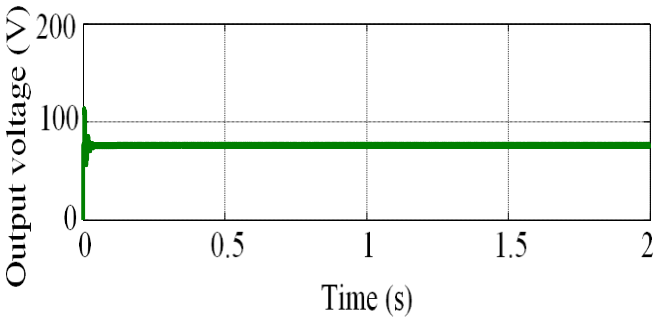

(a) Output voltage.

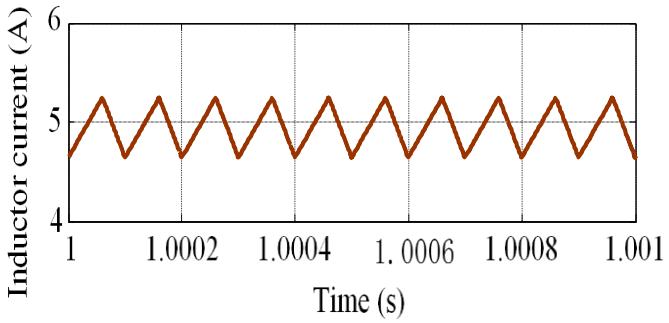

(b) Inductor current.

Fig. 8. Simulation results in buck-boost mode.

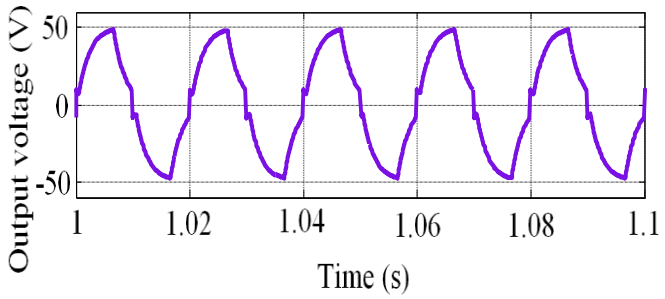

(a) Output voltage.

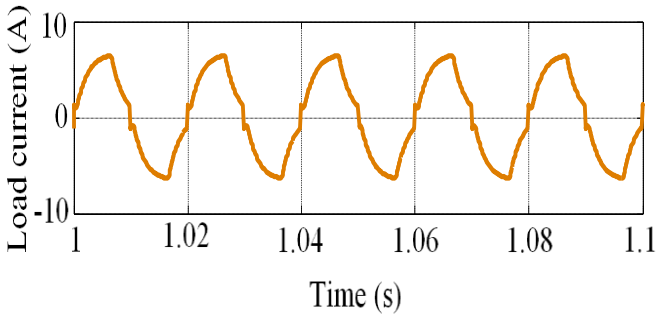

(b) Load current.

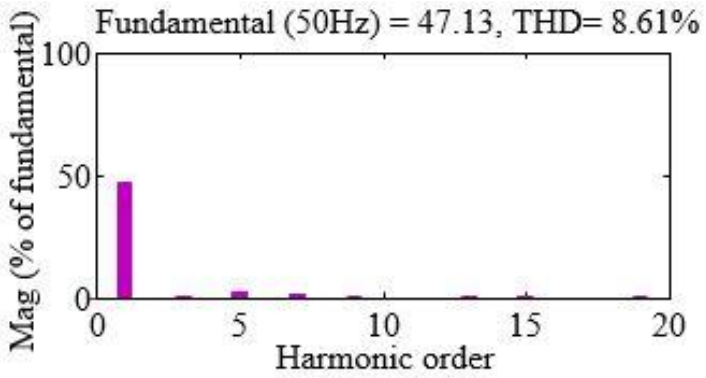

(c) FFT analysis.

Fig. 9. Simulation results in inverter operation.

4.2. Experimental results

In order to verify the effectiveness of the proposed converter, low power prototype circuit is developed in the laboratory. It is tested under the buck, boost, buck-boost and inverter operations. In DC-DC conversion, the test was performed with the input voltage is 50 V, the duty cycle of D = 60%, inductor value is 5 mH, the capacitor is 200 uF and switching frequency 10 kHz is chosen. dSPACE1104 is used as a core controller for generating a controlling signal for active switches IGBT's (STGW30NC120HD). In the buck mode, the experimental output voltage and current flow the inductor are depicted in Figs. 10(a) and (b) respectively. Similarly, output voltage and inductor current in the boost is illustrated in Figs. 11(a) and (b), these are close to the theoretical and simulation results. In addition, output voltage and inductor current in the buck-boost state are shown in Figs. 12(a) and (b) respectively. Afterwards, the proposed converter was tested in inverter configuration, with an input voltage of 50 V and an inductor value is 19 mH, 20 A. Corresponding output voltage load current and FFT analysis are shown in Figs. 13(a), to (c) respectively. Experimental setup developed in the laboratory is shown in Fig. 14.

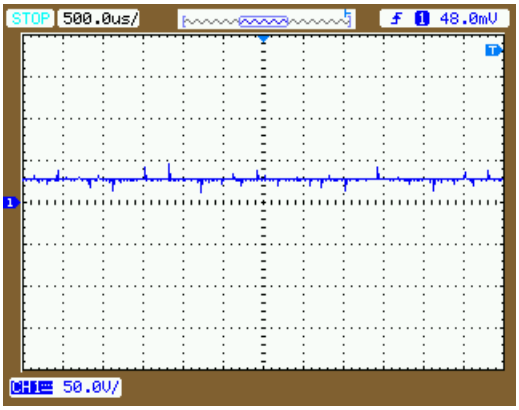

(a) Output voltage (Voltage: 50 V/div, time: 500 us/div).

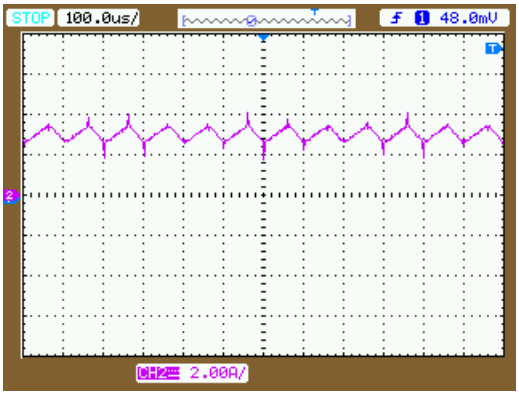

(b) Inductor current (Current: 2 A/div, Time: 100 us/div).

Fig. 10. Experimental results in buck mode.

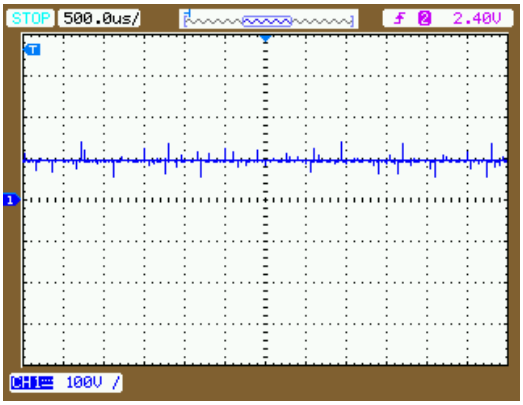

(a) Output voltage (Voltage: 100 V/div, Time: 500 us/div).

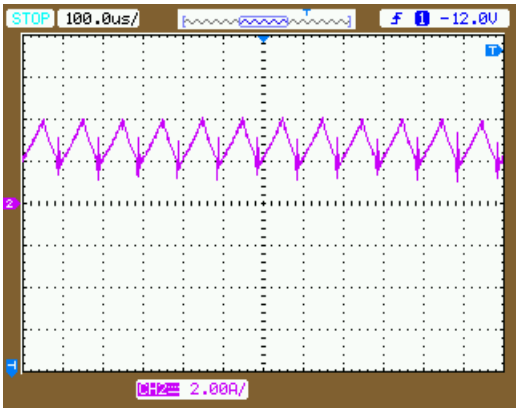

(b). Inductor current (Current: 2 A/div, time: 100 us/div).

Fig. 11. Experimental results in boost operation.

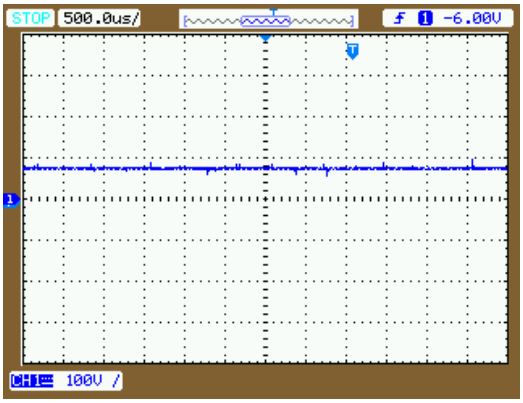

(a) Output voltage (Voltage: 100 V/div, time: 500 us/div).

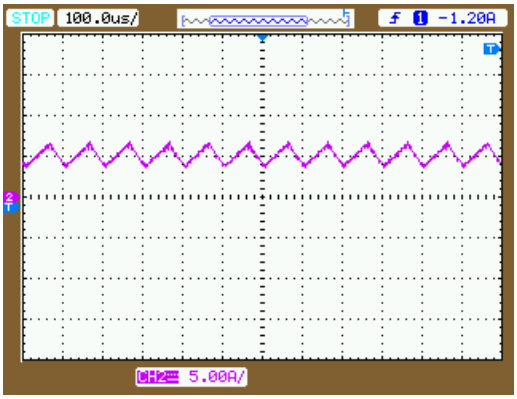

(b) Inductor current (Current: 5 A/div, time: 100 us/div).

Fig. 12. Experimental results in buck-boost operation.

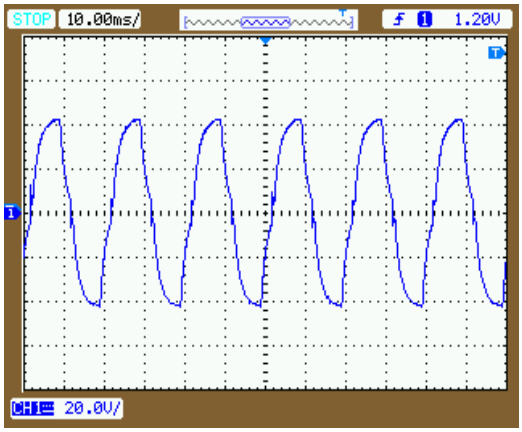

(a) Output voltage (Voltage: 20V/div, Time: 10 ms/div).

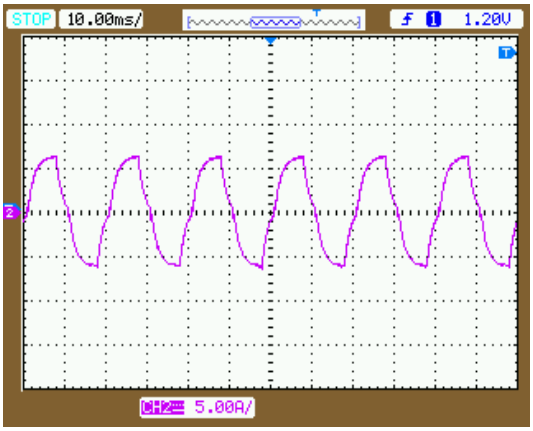

(b) Load current (Current: 5A/div, time: 10 ms/div).

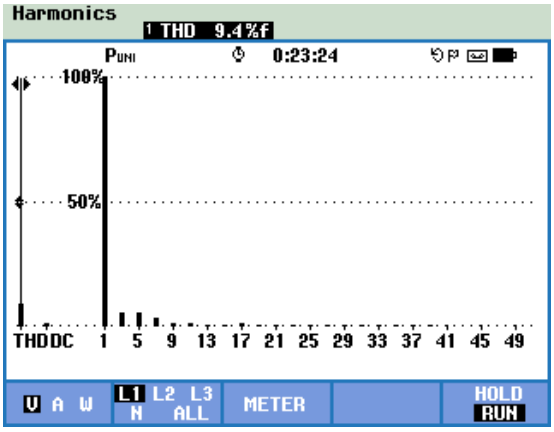

(c) Harmonic spectrum.

Fig. 13. Experimental results in inverter operation.

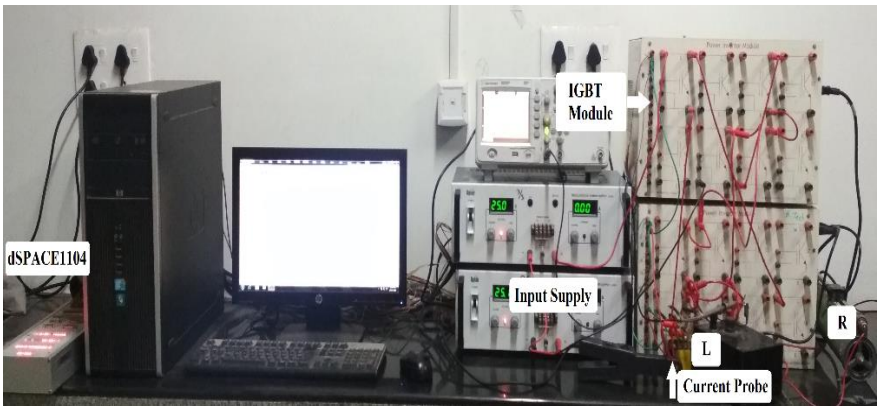

Fig. 14. Experimental setup developed in laboratory.

4. Conclusions

A family of the hybrid converter has been proposed in this paper. The proposed hybrid converter is obtained by combining the traditional DC-DC converter and H-bridge network. The topology, operating principle and different modes of operations are explained in detail. In DC-DC conversion, it can be performed the boost, buck and buck-boost modes, similarly in DC-AC conversion suggested approach is given better THD. Finally, the low power prototype circuit has been developed and experimental results are validated with simulation results.

Nomenclatures

i_L	Inductor current
v_C	Voltage across capacitor
V_{DC}	Input voltage

Abbreviations

EV	Electrical Vehicle
HYC	Hybrid Converter
PFC	Power Factor Correction
THD	Total Harmonic Distortion

References

1. Changchien, S.-K.; Liang, T.-J.; Chen, J.-F.; and Yang, L.-S. (2010). Novel high step-up DC-DC converter for fuel cell energy conversion system. *IEEE Transactions on Industrial Electronics,* 57(6), 2007-2017.
2. Hsieh, Y.-P.; Chen, J.-F.; Liang, T.-J.; and Yang, L.-S. (2017). Novel high step-up DC–DC converter with coupled-inductor and switched-capacitor techniques. *IEEE Transactions on Industrial Electronics,* 59(2), 998-1007.
3. Hwu, K.-I.; and Jiang, W.-Z. (2014). Isolated step-up converter based on flyback converter and charge pumps. *IET Power Electronics,* 7(9), 2250-2257.
4. Banaei, M.R.; and Bonab, H.A.F. (2017). A novel structure for single switch non-isolated transformerless buck-boost DC-DC converter. *IEEE Transactions on Industrial Electronics,* 64(1), 198-205.
5. Shen, H.; Zhang, B.; and Qiu, D. (2017). Hybrid z-source boost DC-DC converters. *IEEE Transactions on Industrial Electronics,* 64(1), 310-319.
6. Tam, K.S.; and Lasseter, R.H. (1987). A hybrid converter for HV DC applications. *IEEE Transactions on Power Electronics,* 2(4), 313-319.
7. Nomura, J.; Kataoka, A.; and Inagaki, K. (2007). Development of a hybrid inverter and a hybrid converter for an electric railway. *Proceedings of Power Conversion Conference*. Nagoya, Japan, 1164-1169.
8. Liu, C.; Gu, B.; Lai, J.-S.; Wang, M.; Ji, Y.; Cai, G.; Zhao, Z.; Chen, C.-L., Zheng, C.; and Sun, P. (2013). High-efficiency hybrid full-bridge–half-bridge converter with shared ZVS lagging leg and dual outputs in series. *IEEE Transactions on Power Electronics*, 28(2), 849-861.
9. Yu, W.; Lai, J.-S., Lai, W.-H.; and Wan, H. (2012). Hybrid resonant and PWM converter with high efficiency and full soft-switching range. *IEEE Transactions on Power Electronics*, 27(12), 4925-4933.
10. Lin, B.-R. (2017). Parallel hybrid converter with wide zero-voltage switching range, less switches and low circulating current losses. *Proceedings of the International Conference on Applied System Innovation (ICASI).* Sapporo, Japan, 1205-1208.
11. Khan, M.A.A.; and Chowdhury, M. (2016). Boost hybrid converter with multiple inductor multiplier cell. *Proceedings of the 3rd Third International Conference on Electrical Engineering and Information Communication Technology (ICEEICT).* Dhaka, Bangladesh, 1-6.
12. Axelrod, B.; Berkovich, Y.; and Ioinovici, A. (2008). Switched-capacitor/switched-inductor structures for getting transformerless hybrid DC-DC PWM converters. *IEEE Transactions on Circuits and Systems: Regular Papers*, 55(2), 687-696.
13. Bagewadi, M.D.; and Dambhare, S.S. (2017). A buck-boost topology based hybrid converter for standalone nanogrid applications. *Proceedings of the IEEE*

2nd International Conference on DC Microgrids (ICDCM). Nuremburg, Germany, 502-506.

14. Harfman-Todorovic, M.; Palma, L.; and Enjeti, P. (2006). A hybrid DC-DC converter for fuel cells powered laptop computers. *Proceedings of the 37th Power Electronics Specialists Conference*. Jeju, South Korea, 1-5.
15. Dogga, S.; Surendar, V.; Ponnambalam, P.; and Kumar, M.P. (2015). Boost derived hybrid converter implementation using fuzzy controller. *Proceedings of the International Conference on Technological Advancements in Power and Energy (TAP Energy)*. Kollam, India, 381-386.
16. Siddhartha, V.; and Hote, Y.V. (2016). Non-inverting buck-boost derived hybrid converter. *Proceedings of the International Conference on Emerging Trends in Electrical Electronics and Sustainable Energy Systems (ICETEESES)*. Sultanpur, India, 234-240.
17. Tomy, A.; and Thomas, A.J. (2016). Sepic derived hybrid converter with simultaneous AC and DC outputs. *Proceedings of the IEEE Annual India Conference (INDICON)*. Bangalore, India, 1-6.
18. Sarath, R.; and Kanakasabapathy, P. (2015). Switched-capacitor/switched-inductor cuk-derived hybrid converter for nanogrid applications. *Proceedings of the 4th International Conference on Computation of Power, Energy, Information and Communication (ICCPEIC)*. Melmaruvathur, India 430-434.
19. Kim, J.-H.; Lee, II.-O.; and Moon, G.-W. (2017). Analysis and design of a hybrid-type converter for optimal conversion efficiency in electric vehicle chargers. *IEEE Transactions on Industrial Electronics*, 64(4), 2789-2800.
20. Kim, Y.-D.; Lee, II.-O.; Choo, I.-H.; and Moon, G.-W. (2014). Hybrid dual full-bridge DC–DC converter with reduced circulating current, output filter, and conduction loss of rectifier stage for RF power generator application. *IEEE Transactions on Power Electronics*, 29(3), 1069-1081.
21. Zhang, J.; Zhao, C.; Zhao, S.; and Wu, X. (2017). A family of single-phase hybrid step-down PFC converters. *IEEE Transactions on Power Electronics*, 32(7), 5271-5781.
22. Vecchia, M.D.; Salvador, M.A.; and Lazzarin, T.B. (2017). Hybrid non-isolated DC-DC converters derived from a passive switched-capacitor cell. *IEEE Transactions on Power Electronics*, 33(4), 3157-3168.
23. Kazimierczuk, M.K. (2008). *Pulse-width modulated DC-DC power converters* (1st ed.). West Sussex, United Kingdom: John Wiley and Sons, Ltd.